minerals

MDPI

Essay

Study on the Properties of Vanadium Pellets Extracted from Vanadium Titanium Magnetite Concentrate by Calcium Roasting and Acid Leaching

Yang Li [1], Zhonghui Peng [1,2], Zhixiang Wang [1], Yongze Zhu [1] and Keqiang Xie [1,*]

[1] Faculty of Metallurgical and Energy Engineering, Kunming University of Science and Technology, Kunming 650093, China
[2] Sichuan Lomon Mining and Metallurgy Co., Ltd., Panzhihua 617100, China
* Correspondence: xkqzhh@sina.com

Abstract: In this study, a clean pellet production method of calcium roasting and sulfuric acid leaching of vanadium from vanadium and titanium magnetite concentrates is proposed, which can effectively separate vanadium and iron, and the pellets after acid leaching and vanadium extraction can be used as raw material for iron making after secondary roasting. During the experiment, only 2% $Ca(OH)_2$ was added as the calcifier to make pellets, and vanadium was extracted by acid leaching after calcination. Under the optimum conditions, the vanadium leaching rate was 74.51%, and the iron leaching rate was only 1.05%. After secondary roasting, the compressive strength of the pellets was 2358 N, and the qualification rate was 97%. Additionally, after acid leaching and vanadium extraction, the impurities in the pellet were partially removed, and the iron content of the pellet increased by 6.6%, which is more conducive to subsequent ironmaking. The roasting and acid leaching experiments show that based on the production of iron smelting pellets, the use of pellets can better extract vanadium from the titanium magnetite concentrate, while avoiding the problems of excessive additives to reduce the iron grade of pellets. Or the pursuit of high vanadium extraction rate pellets, which can be seriously damaged and difficult to use later. This process can perform a comprehensive utilization of vanadium titanium magnetite, and has certain guiding significance for industrial production.

Keywords: vanadium-titanium iron concentrate pellets; calcium roasting; acid dip vanadium; vanadium leaching rate; iron concentrate pellet properties

check for updates

Citation: Li, Y.; Peng, Z.; Wang, Z.; Zhu, Y.; Xie, K. Study on the Properties of Vanadium Pellets Extracted from Vanadium Titanium Magnetite Concentrate by Calcium Roasting and Acid Leaching. *Minerals* **2023**, *13*, 399. https://doi.org/10.3390/min13030399

Academic Editor: Rajesh Kumar Jyothi

Received: 19 February 2023
Revised: 5 March 2023
Accepted: 9 March 2023
Published: 14 March 2023

Copyright: © 2023 by the authors. Licensee MDPI, Basel, Switzerland. This article is an open access article distributed under the terms and conditions of the Creative Commons Attribution (CC BY) license (https://creativecommons.org/licenses/by/4.0/).

1. Introduction

In recent years, with the depletion of iron ore resources, its comprehensive utilization has aroused people's interest, and therefore it has been widely studied [1]. Vanadium titanium magnetite is rich in iron, vanadium, titanium, and other valuable metal elements, while vanadium is widely used as an important strategic resource [2,3]. It is mainly used in the metallurgical industry, machinery manufacturing, batteries, chemical industry, and aerospace [4–6]. In terms of energy storage, the vanadium flow battery has attracted much attention due to several advantages such as its long cycle life, high energy efficiency, and large-scale energy storage [7].

At present, vanadium is mainly extracted from vanadium slag [8]. Vanadium exists in vanadium slag in the form of vanadium spinel, which is very stable, and therefore it is difficult to directly leach vanadium from it [9]. In the roasting process, alkaline salt is added to convert vanadium into leachable vanadate, and vanadium can then be extracted from aqueous solution [10]. Using this process, some vanadium will enter molten iron in the blast furnace ironmaking, and the subsequent vanadium extraction rate is low, which causes high pollution to the environment [11–13]. The vanadium leaching rate of the process of first extracting vanadium and then ironmaking is relatively high, and therefore

it has been widely studied [14,15]. For instance, Li et al. [16] used potassium salt roasting to leach vanadium. And the sodium roasting–water leaching process [17]. The roasting process will produce HCl, Cl_2, and other harmful gases, and the vanadium extraction residue containing high sodium is difficult to use [18,19]. Similarly, the leaching rate of vanadium by salt-free roasting is low [20]. These processes all have the same limitation, that is, they neglect the treatment of tailings. However, calcium salt roasting converts low-valence vanadium into high-valence calcium vanadate, which is insoluble in water. Through acid leaching, it can then selectively separate ferrovanadium without producing harmful gases. This proved to be an efficient process. Moreover, the high selectivity of calcium salts for vanadium allows all chromium to remain in the iron ore concentrate, enabling the complete separation of vanadium and chromium [21]. The calcium roasting and acid leaching process of Luo [22] can better extract vanadium. However, it has some limitations. For example, the excessive calcium salt addition reduces the iron grade of pellets, which is not conducive to subsequent iron smelting, and the acid consumption of calcium sulfate precipitation generated in the acid leaching process increases.

The vanadium content of the vanadium titanium magnetite concentrate provided in this experiment was only 0.3%. It is difficult to use the process of iron smelting before vanadium extraction for subsequent treatment. Therefore, in order to better recover vanadium, our team used the process of vanadium extraction followed by iron-making. As one of the main sources of the ironmaking process, pellets have attracted much attention due to their high performance [23]. Therefore, this study tackles the process of pelletizing vanadium from vanadium titanium magnetite concentrate. While increasing the vanadium leaching rate, appropriate calcifying agents are used to reduce the additive content in the pellets and simultaneously reduce the pellet damage rate in the roasting acid leaching process, so that the pellets after vanadium extraction can be directly used as iron smelting pellets after simple treatment.

2. Experimental

2.1. Materials

The vanadium titanium magnetite concentrate provided by a company in Panzhihua is considered the research object. The vanadium titanium magnetite concentrate is ground to the required particle size. The chemicals used in the experiments, calcium hydroxide ($Ca(OH)_2$) and sulfuric acid (H_2SO_4), were of analytical grade.

2.2. Test Procedure

The whole experimental process is shown in Figure 1.

The vanadium titanium magnetite concentrate is ground and dried, and 1 kg is weighed each time. A certain amount of bentonite and calcium hydroxide is added into the crucible to mix for 15 min. The balls are made on an 800 mm × 165 mm disc ball-making machine with an inclination angle of 48° and a speed of 21 r/min. 6%–10% water is then added to the pelletizing process. After pelletizing, a pellet is selected with a diameter of 10–16 mm and no obvious crack grooves and protrusions to dry at 105 °C for 2 h for standby. In each experiment, 200 ± 2 g of pellets are weighed and put into a muffle furnace for roasting. The roasting temperature range is 900–1300 °C, and the time is between 0 h and 3 h. After roasting, the pellets are naturally cooled to room temperature, and the pellets are taken out to determine their performance, while the subsequent acid leaching experiments are pending. For each experiment, 100 ± 1 g of roasted pellets is weighed into a beaker in a water bath pan, and reactions are performed under different temperatures, acid concentrations, liquid–solid ratios, and time conditions. After leaching, a liquid–solid separation of reactants is performed and the vanadium leaching efficiency is calculated. After cleaning the pellets to remove residues, secondary roasting is performed to obtain qualified ironmaking raw materials.

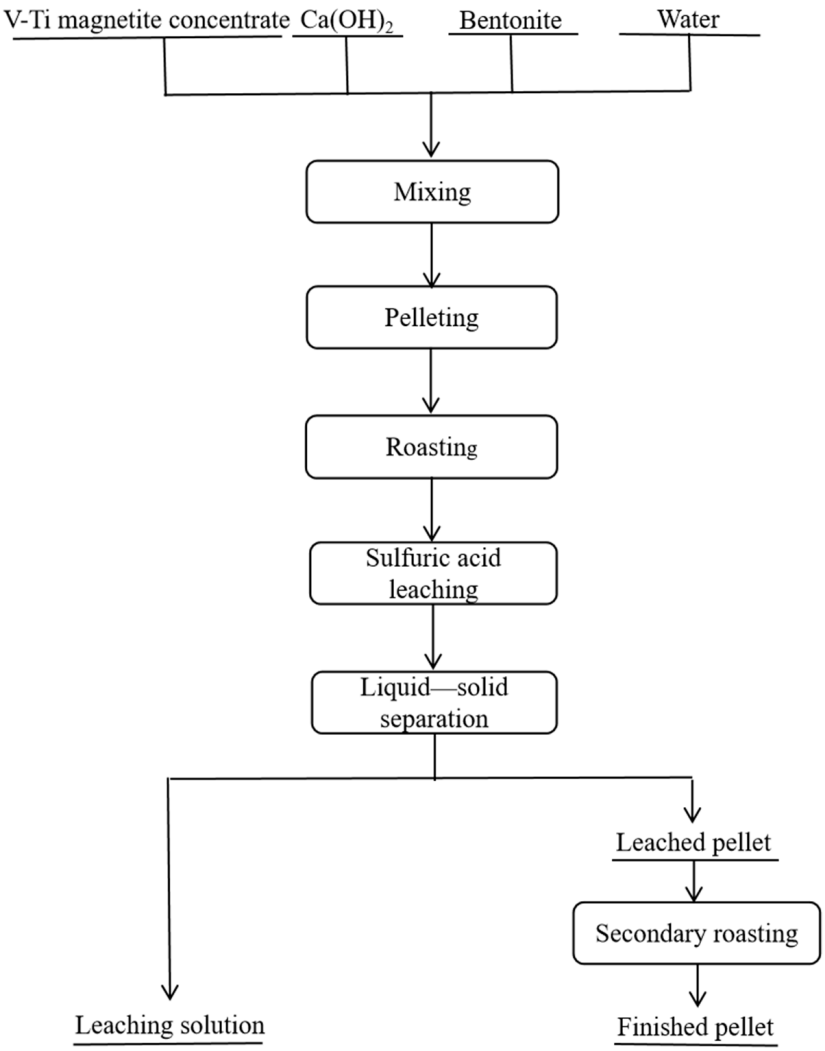


Figure 1. Flow chart of calcification roasting–sulfuric acid leaching method.

2.3. Analytical Methods

The chemical composition of raw ore and secondary roasted pellets was analyzed by the inductively coupled plasma optical emission spectrometer (ICP-OES). X-ray diffraction (XRD) was used to analyze the phase composition of raw ore and roasted pellets. Scanning electron microscopy and energy dispersive X-ray spectroscopy (SEM-EDS) was used to observe the element distribution of raw ore, calcined pellets, leached pellets, and secondary roasted pellets. The compressive strength of pellets was tested using a digital display pellet pressure tester (KYS-10, Jinan Testing Instrument Factory, China). The content of Fe and V was tested using an inductively coupled plasma optical emission spectrometer (ICP-OES). Additionally, the porosities of the pellets were measured with a mercury injection apparatus (JK-YG2000, Jingkerida, China).

3. Results and Discussion

3.1. Concentrate Characteristics

The chemical composition of vanadium titanium magnetite concentrate is shown in Table 1. The iron grade is 52%, and the vanadium grade is only 0.3%. Therefore, the separation of Fe and V is crucial. As can be seen from Figure 2, the phase analysis of vanadium titanium magnetite concentrate shows that Fe in the raw ore mainly exists in the form of Fe_3O_4 and $FeTiO_3$, and the vanadium content is less than 1%, and therefore it cannot be detected.

Table 1. Chemical compositions (ICP) of vanadium magnetite concentrate.

Element	Fe	Ti	Si	Ca	Mg	V	Ni	Na	S	Cl
Content (wt.%)	52.00	9.00	2.00	0.60	0.40	0.30	0.10	0.03	0.80	0.20

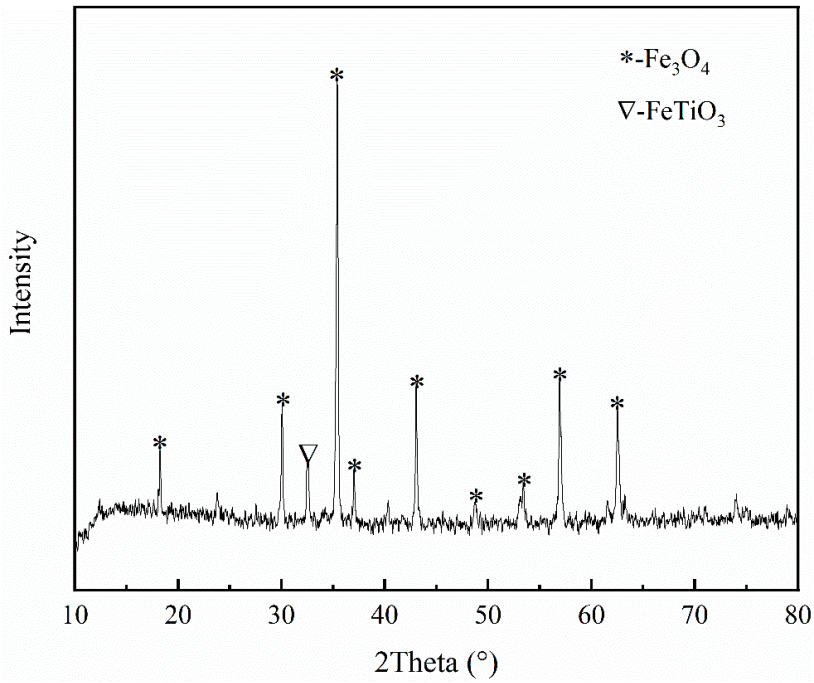


Figure 2. XRD pattern of V-Ti magnetite concentrate.

3.2. Experimental Results of Pelleting Experiments

The experiments first investigated the effects of the percentage of mineral powder of −0.074 mm particle size, the addition of calcium hydroxide, bentonite content, and granulation time on the performance of raw pellets. After pelletizing, pellets with diameters of 8–16 mm were selected, and the effects of various factors on the falling strength, compressive strength, and bursting temperature of raw pellets were measured. In each experiment, 14 pellets were selected, and the drop strength and compressive strength of raw pellets were measured. After the measurement results, the two highest values and two lowest values were removed, and the average value of the remaining values was taken. The experiment was repeated once to observe the difference between the two experimental results, whether the drop strength difference was ≤ 1 time, and the compressive strength difference was ≤ 10 N. If the requirements were met, the average of the two results was used as the compressive strength of the particles, and if not, the measurement was repeated. For the raw ball burst temperature, the dynamic method proposed by the U.S. company in a vertical tube furnace was used; 50 raw balls were loaded into a stainless steel tank; hot airflow was passed at a certain speed through the raw ball layer; the raw balls in the chamber were left for 5 min, and then removed; for each experiment, the temperature increased by 10 °C to 4% of the raw ball rupture temperature defined as the raw ball burst temperature and was repeated twice to take the average.

It can be seen from Figure 3a that when the proportion of −0.074 mm particle size of iron concentrate increases from 50% to 70%, the falling strength of green pellets shows an upward trend. This is due to the fact that when the particle size gradually decreases, the green pellet structure becomes more compact, and the falling strength of pellets reaches its highest value when the proportion is 70%. When the particle size of iron concentrate further increases, the falling strength of the pellets shows a downward trend. The particle structure of the irregular, needle-shaped iron concentrate is damaged with the extension

of the ball milling time. At this time, the particle size distribution of the iron concentrate is not conducive to balling, and the falling strength of the green pellets decreases. The compressive strength of green pellets will continuously increase when the particle size becomes smaller. When the particle size of −0.074 mm accounts for 70%, the compressive strength exceeds 50 N. When the particle size increases, the bursting temperature of green pellets decreases and the porosity of the pellets becomes small. When the particle size of −0.074 mm accounts for more than 70%, the bursting temperature of the green pellets slightly increases. This is due to the fact that with further refinement of the iron concentrate particle size, the water content required in the pelleting process decreases, and the bursting temperature of green pellets is improved. It is most appropriate to consider that the iron concentrate accounts for almost 80% of the total iron concentrate.

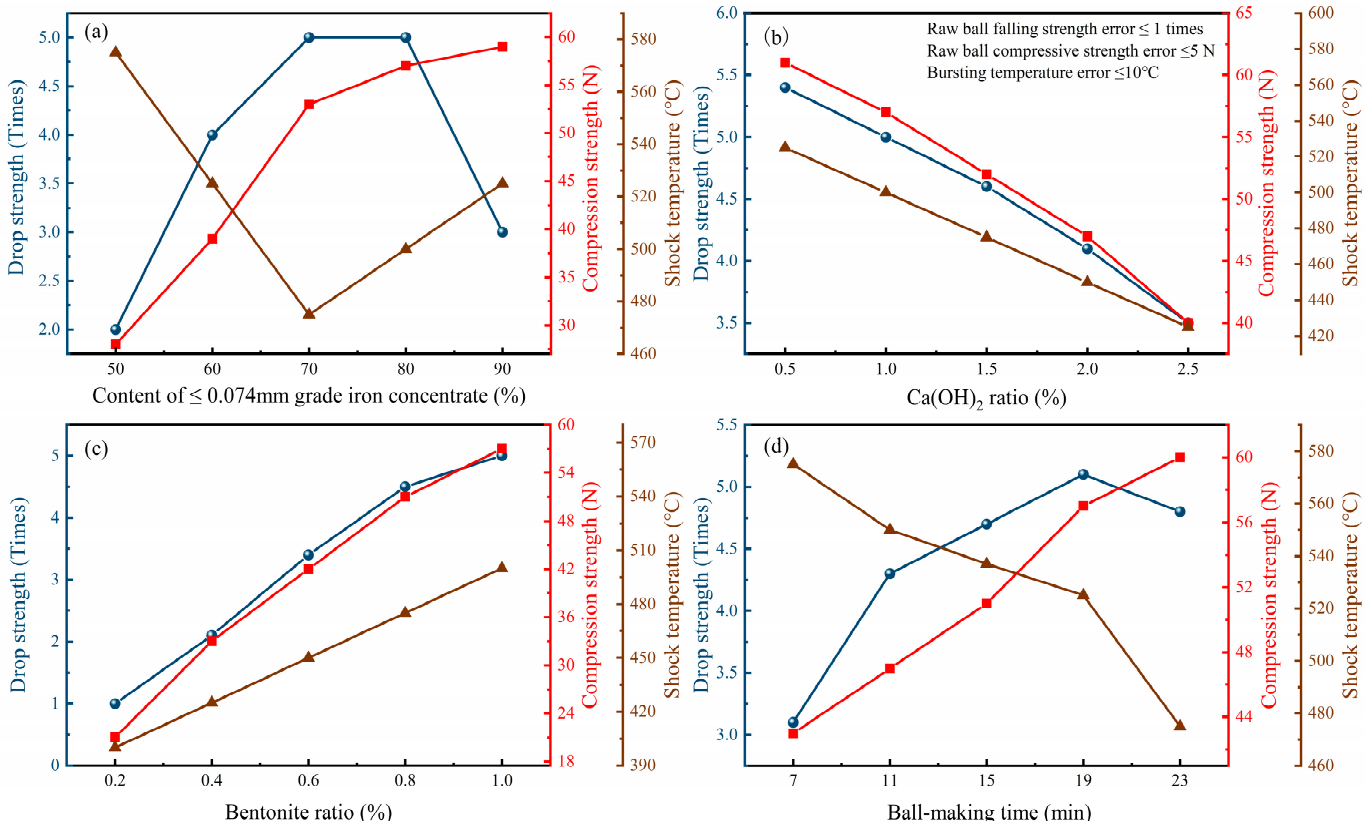


Figure 3. Effect of pelletizing factors on raw ball drop strength, compressive strength, bursting temperature. (**a**) the effect of iron concentrate −0.074 mm particle size ratio; (**b**) the effect of $Ca(OH)_2$ ratio; (**c**) the effect of bentonite ratio; (**d**) the effect of ball-making time.

In the experiment, calcium hydroxide was mainly used as a calcifier for the subsequent acid leaching of vanadium. It can be seen from Figure 3b that when the calcium hydroxide content increases, the falling strength, compressive strength, and bursting temperature of the green pellets show a downward trend. Therefore, the amount of calcium hydroxide should be reduced as much as possible to meet the requirements of vanadium extraction. The actual amount of calcium hydroxide should be determined according to the subsequent baking test and vanadium extraction effect.

As the binder of pellets, bentonite significantly affects the strength of pellets. It can be seen from Figure 3c that when the bentonite content increases from 0.2% to 1%, the falling strength, compressive strength, and bursting temperature of the green pellets show an upward trend. However, too much bentonite will reduce the iron grade of the pellets, and the effect of vanadium extraction is poor if the pellets are too dense. The added amount should depend on the subsequent pellet performance and vanadium extraction effect.

The pelleting time was controlled from 7 to 23 min. It can be seen from Figure 3d that, when the ball-making time increases, the falling strength of green pellets shows an upward trend, and continued to extend the pelleting time to 19 min; the falling intensity of green pellets decreased. At this time, the water on the pellet surface evaporates, and the bonding property becomes worse. With the extension of pelleting time, the compressive strength of green pellets increases continuously, and the pellet structure is more compact, so the burst temperature will continue to drop. Moreover, a too-long pelleting time will lead to a decline in the yield, so a reasonable pelleting time should be about 19 min.

3.3. Results of Roasting Experiments

The roasting temperatures were then set to 800 °C, 900 °C, 1000 °C, 1100 °C, 1200 °C, and 1300 °C. The effects of roasting time, calcium hydroxide content and bentonite content on the compressive strength of pellets and vanadium leaching rate were investigated. The leaching temperature, leaching time, liquid–solid ratio and sulfuric acid concentration were 1 h, 1%, 1%, 90 °C, 3d, 1:1, and 3.5 mol/L. Fourteen pellets with diameters of 8–16 mm were selected for each experiment and the compressive strength of the pellets was measured. The two highest and two lowest values were removed after the measurement results and the average of the remaining values was taken and the experiment was repeated once, observing the difference between the two experimental results ≤100 N. If the requirements were met, the average of the two results was taken as the compressive strength of the pellet, and the measurement was repeated if it was excessive. For each leaching experiment 100 ± 1 g of pellets were selected to be leached in acid solution according to the experimental conditions and the vanadium leaching rate was calculated after leaching. The test results are shown in Figure 4.

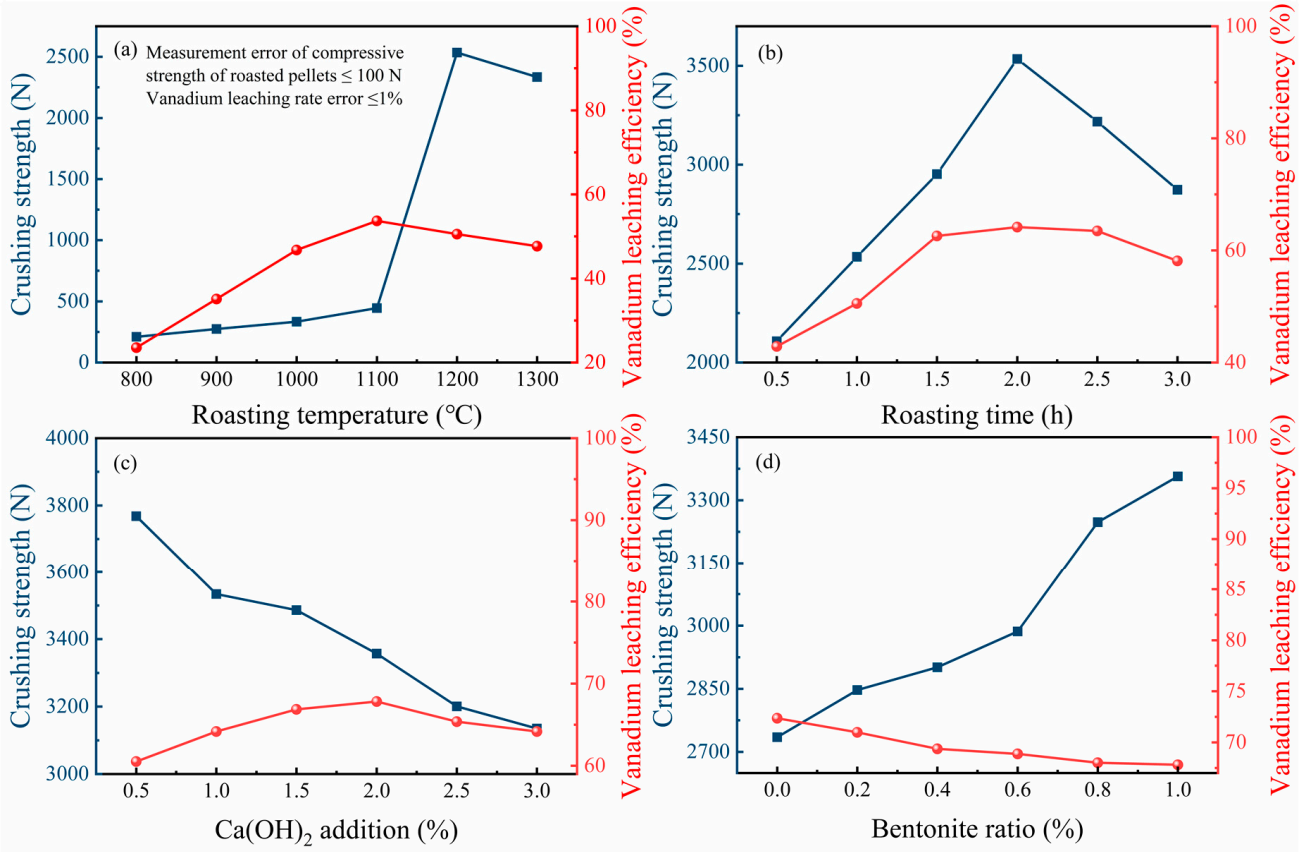


Figure 4. Effect of roasting factors on pellet compressive strength and vanadium leaching rate. (**a**) Effect of roasting temperature; (**b**) Effect of roasting time; (**c**) Effect of calcium hydroxide addition; (**d**) Effect of bentonite addition.

It can be seen from Figure 4a that, when the temperature increases, the compressive strength of the pellets slowly increases at 900–1100 °C, which is only almost 500 N. When the temperature becomes greater than 1100 °C, the compressive strength of the pellets sharply increases and reaches its highest value of 2756 N at 1200 °C. When the temperature increases to 1300 °C, the compressive strength of the pellets decreases. At this time, the pellets are stuck due to over melting, and the energy consumption in the actual process is too high, which is not conducive to the production of pellets. Figure 5 shows the XRD diagrams of pellets calcined at different temperature gradients. It can be observed that iron in raw ore mainly exists in the form of Fe_3O_4. After calcination, iron is oxidized, and ferrous iron is converted into ferric iron. In addition, Fe_2TiO_5 diffraction peaks appear, which are the product of the reaction between Fe_2O_3 and TiO_2 [24]. When the roasting temperature reaches 1300 °C, a diffraction peak of silicate is observed, which is not conducive to the consolidation of pellets and the leaching of vanadium. The degree of calcium vanadate generated from pellet roasting is related to the subsequent vanadium leaching effect with sulfuric acid solution.

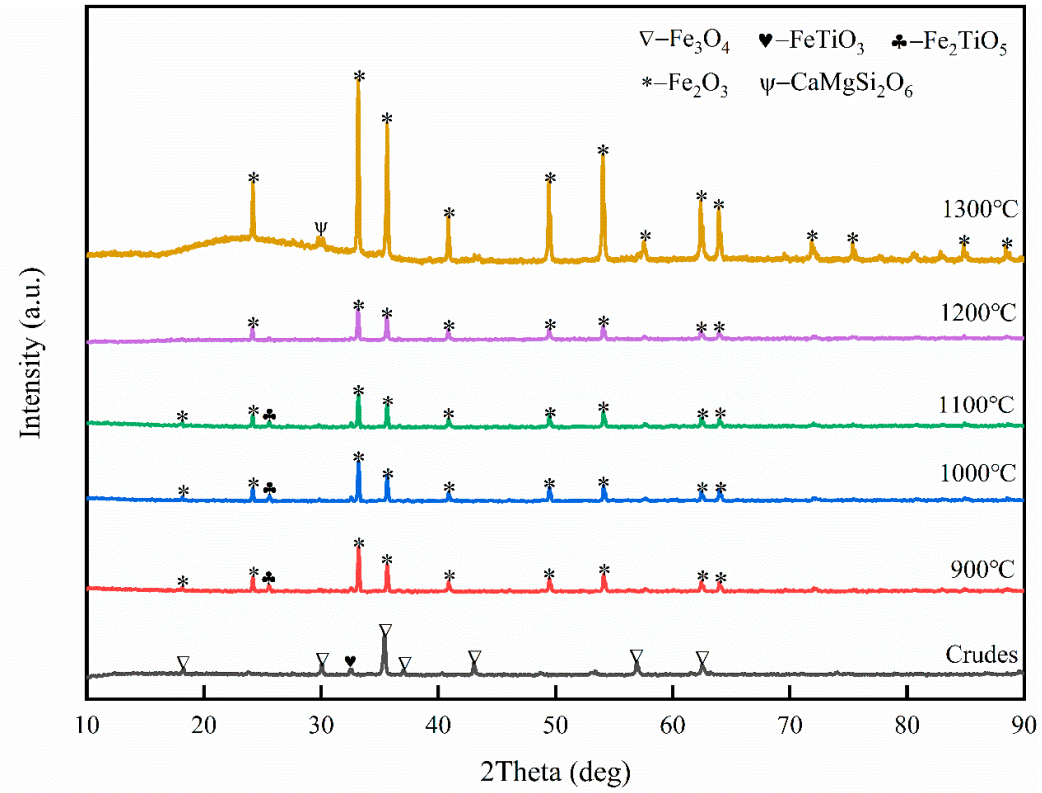


Figure 5. XRD pattern of pellet samples.

It can be seen from Figure 4a that the vanadium leaching rate is only 23.18% when roasting at 800 °C, and it can reach 53.31% (which is the highest value) when the temperature increases to 1100 °C. When the roasting temperature is higher than 1100 °C, the pellet strength rapidly increases, the V leaching is hindered, and the leaching rate significantly decreases. When the temperature is higher than 1200 °C, the pellets will generate new inclusions, which will prevent the leaching of vanadium. Zheng et al. [25] showed that when molten silicate is generated during the roasting of magnetite, it will hinder the conversion of V^{3+} to V^{5+}, making the V oxidation incomplete and reducing the leaching efficiency. Moreover, the structure of pellets will be damaged during acid leaching, and the surface will crack or break; therefore, the compressive strength of baked pellets should be improved as much as possible.

Figure 4b shows the effect of different roasting times on the compressive strength and vanadium leaching rate of the pellets. When the roasting time was increased from 0.5 to

2 h, the compressive strength of the pellets continued to increase and the highest strength was obtained at 2 h. The compressive strength of the pellets tended to decrease as the roasting time continued to increase. The leaching rate of vanadium increased continuously between 0.5 and 1.5 h. The increase in the vanadium leaching rate was not significant when extended to 2.5 h. A continued extension of the roasting time resulted in a decrease in the vanadium leaching rate. Below the optimum roasting time, the consolidation of pellets and the oxidation state of vanadium are not sufficient. Beyond the optimum roasting time, low melting point calcium salts will be produced within the pellet to encapsulate the vanadium, which inhibits the oxidation of vanadium, making subsequent leaching by sulfuric acid difficult. When the roasting time is 2 h, the reaction in the pellet is more complete, the pellet has the highest compressive strength, and the vanadium leaching rate can reach 64.31%.

Figure 4c shows the influence of different calcium hydroxide ratios on the compressive strength of pellets and vanadium leaching rate. When the $Ca(OH)_2$ content continuously increases, the compressive strength of pellets continues to decrease. The vanadium leaching rate continues to increase before 2% and when it exceeds 2%, the vanadium leaching rate will gradually decrease. Calcium hydroxide decomposes and absorbs heat during roasting to inhibit the consolidation of pellets, and excessive calcium hydroxide is added to generate a low melting point calcium salt, which has adverse effects on the compressive strength of pellets. Moreover, due to the low vanadium content, excessive calcium salt is added during the experiment to make it easier to react and generate calcium vanadate. However, if too much calcium salt is added, it will react with sulfuric acid in the acid leaching process, generating calcium sulfate precipitation and consuming a large amount of sulfuric acid solution. Therefore, 2% calcium hydroxide is the most appropriate addition to the pellet.

Figure 4d shows the influence of different bentonite ratios on the compressive strength and vanadium leaching rate of pellets. When the bentonite content increases from 0% to 1%, the compressive strength of the pellets continues to increase, while the vanadium leaching rate shows a downward trend. This is because bentonite makes the particles in the pellet bond firmer, but it also hinders the leaching of vanadium. Too much bentonite will also reduce the iron grade of pellets. Therefore, 0.8% bentonite is the most appropriate amount to ensure that the roasted pellets still have a high performance to meet the requirements of iron smelting after acid leaching.opp

The reaction in the roasting process for a temperature range of 0–1300 °C, in the case of 2% calcium hydroxide added to the pellets, is described in the sequel. Note that the relevant data are calculated using the FactSage software.

$$Ca(OH)_2 = CaO + H_2O \quad (1)$$

$$4FeV_2O_4 + O_2 = 2Fe_2O_3 + 4V_2O_3 \quad (2)$$

$$2V_2O_3 + O_2 = 2V_2O_4 \quad (3)$$

$$2V_2O_4 + O_2 = 2V_2O_5 \quad (4)$$

$$V_2O_5 + CaO = Ca(VO_3)_2 \quad (5)$$

$$V_2O_5 + 2CaO = Ca_2V_2O_7 \quad (6)$$

$$V_2O_5 + 3CaO = Ca_3(VO_4)_2 \quad (7)$$

$$4Fe_3O_4 + O_2 = 6Fe_2O_3 \quad (8)$$

$$4FeTiO_3 + O_2 = 2Fe_2O_3 + 4TiO_2 \quad (9)$$

$$Fe_2O_3 + TiO_2 = Fe_2TiO_5 \quad (10)$$

$$CaO + MgO + 2SiO_2 = CaMgSi_2O_6 \quad (11)$$

As can be seen in Figure 6, the ΔG^{θ} for reactions (2) to (11) are negative in the temperature range 0–1300 °C, indicating that these reactions are thermodynamically feasible. Reaction (1) is the reaction equation for the additive $Ca(OH)_2$, which also has a negative

value of ΔG^{θ} after 500 °C, indicating that $Ca(OH)_2$ is thermally decomposed at this time. Reactions (2) to (9) indicate the conversion of Fe^{2+} to Fe^{3+} during roasting and the further reaction of vanadium with calcium oxide to form calcium vanadate. In addition, reaction (11) indicates that silica can react with calcium to form silicate, which is not favorable for subsequent acid leaching.

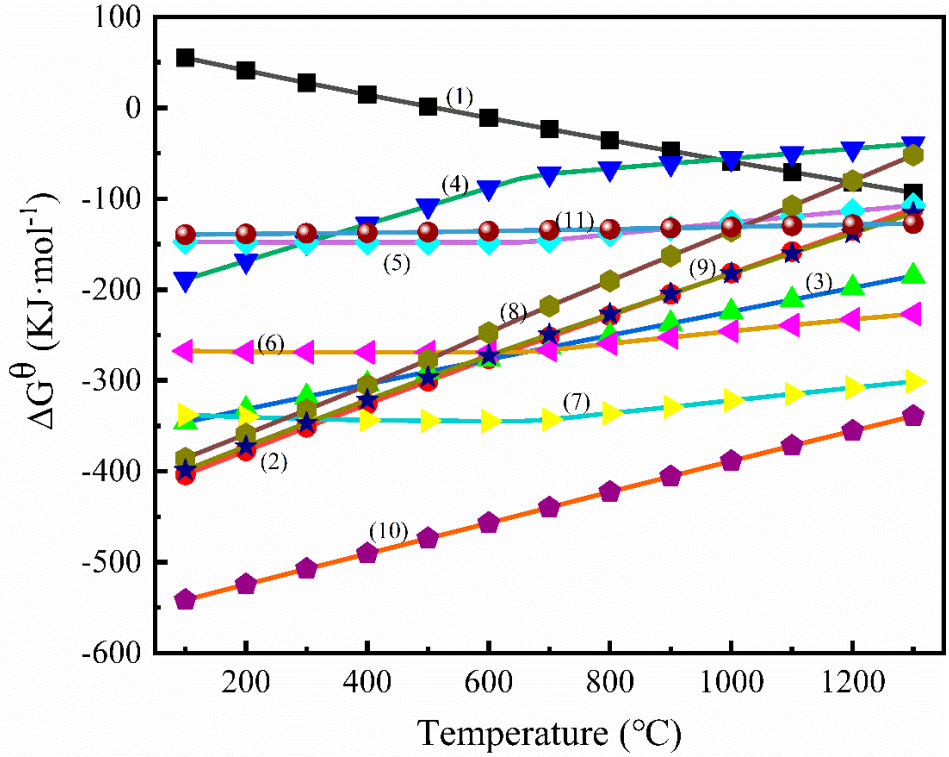


Figure 6. $\Delta G^{\theta}-T$ diagrams for possible chemical reactions (Equations (1)–(11)).

3.4. Results of Leaching Experiments

Under the optimum conditions of roasting at 1200 °C, a roasting time of 2 h, the addition of 2% calcium hydroxide and a bentonite proportion of 0.8%. The effects of acid leaching temperature, acid concentration, liquid–solid ratio, and leaching time on the leaching rate of ferrovanadium from pellets were investigated and the results are as follows.

The leaching temperature was set to 15 °C, 30 °C, 45 °C, 60 °C, 75 °C, and 90 °C, with acid concentration, liquid–solid ratio, and a leaching time of 3 mol/L, 1:1, and 3 d, respectively. The impacts of different leaching temperatures on the leaching rate of vanadium and iron were studied. The test results are shown in Figure 7a. When the leaching temperature increases from 30 °C to 90 °C, the V leaching rate rapidly increases from 20.68% to 64.31%, and the iron leaching rate has little change. However, when the temperature is too high during acid leaching, the evaporation rate of the acid solution is high, and the pellets can easily break after acid leaching. Therefore, 80 °C was finally determined as the optimal leaching temperature.

Figure 7b shows the impacts of different acid concentrations on the vanadium and iron leaching rates. When the concentration of sulfuric acid increases from 1 mol/L to 3.5 mol/L, the vanadium leaching rate generally shows a trend of first increasing and then decreasing. When the concentration of sulfuric acid is 3 mol/L, the vanadium leaching rate reaches its maximum value, and the optimal leaching rate is 64.31%. The vanadium leaching rate does not significantly increase with the increase in the acid concentration. When the sulfuric acid concentration increases, the leaching rate of iron increases from 0.18% to 1.52%. The optimal sulfuric acid concentration is set to 3 mol/L in order to reduce its consumption.

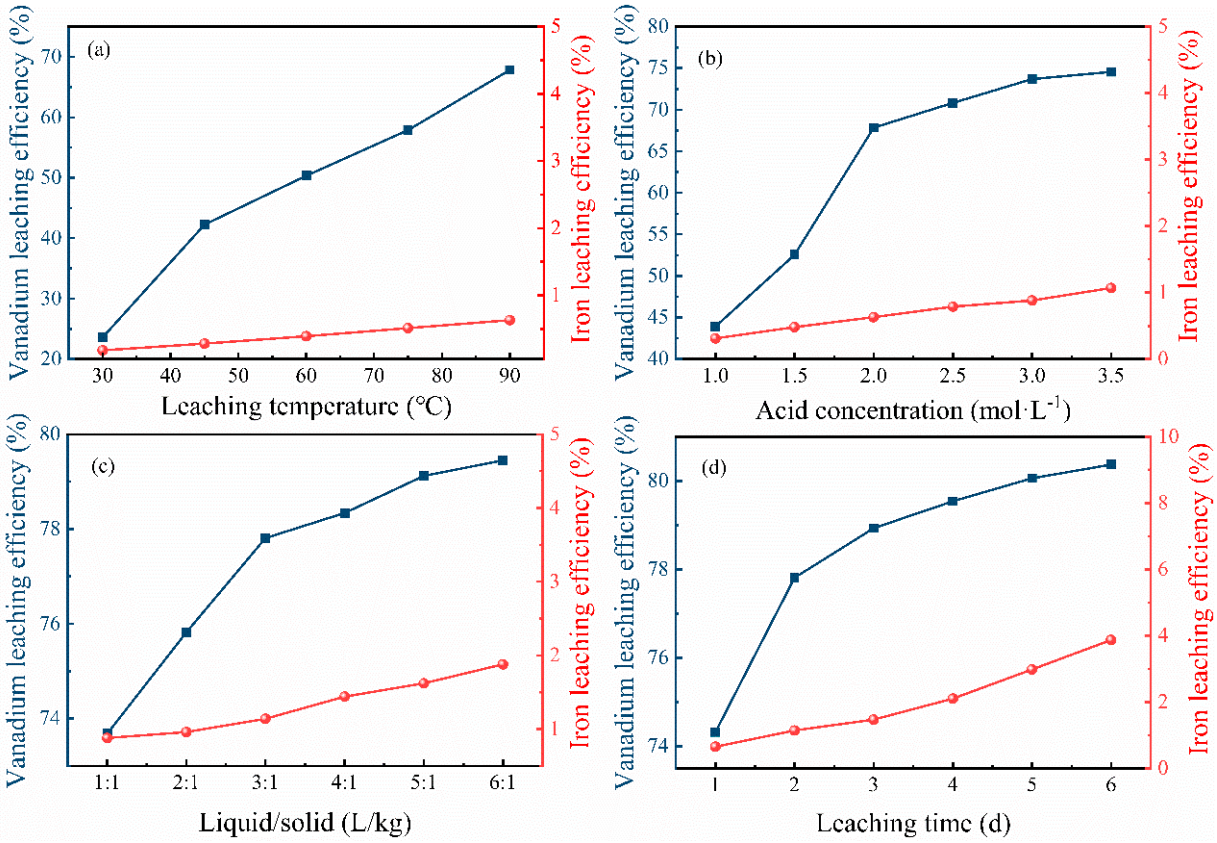


Figure 7. Effect of acid leaching factors on the leaching rate of vanadium and iron from pellets. (**a**) Effect of leaching temperature; (**b**) Effect of acid concentration; (**c**) Effect of liquid-solid ratio; (**d**) Effect of leaching time.

Figure 7c shows the impacts of different liquid–solid ratios on the vanadium and iron leaching rates. When the liquid–solid ratio increases, the vanadium leaching rate continuously increases. When the liquid–solid ratio is 3:1, the vanadium leaching rate reaches 74.51%. If the liquid–solid ratio continues to increase, the vanadium leaching rate will not significantly increase. In addition, the higher the liquid–solid ratio, the higher the consumption of sulfuric acid, and the lower the vanadium concentration in the leaching solution, which is not conducive to the recovery of vanadium in the subsequent process. Therefore, in order to reduce the acid consumption, the optimal liquid–solid ratio is set to 3:1. At this time, the leaching rate of iron is less affected by the liquid–solid ratio. For a liquid–solid ratio of 3:1, only 1.08% of the iron is leached, which indicates that vanadium and iron can achieve efficient selective separation.

Figure 7d shows the influence of the leaching time on the vanadium and iron leaching rates. When the leaching time increases from 1 d to 6 d, the vanadium leaching rate increases. After 3 d of leaching, the leaching rate of vanadium tends to be flat. As for iron leaching, although the overall trend is increasing, the overall leaching rate is lower than 1.5%. Therefore, the optimal leaching time is determined as 3 d. The reaction between calcium vanadate and sulfuric acid during acid leaching is summarized in the sequel.

The reaction of calcium metavanadate, calcium orthovanadate, calcium pyrovanadate, and sulfuric acid produced by the calcined pellets is shown in (12)–(14).

$$Ca(VO_3)_2 + 2H_2SO_4 = (VO_2)_2SO_4 + CaSO_4 + 2H_2O \quad (12)$$

$$Ca_2V_2O_7 + 3H_2SO_4 = (VO_2)_2SO_4 + 2CaSO_4 + 3H_2O \quad (13)$$

$$Ca_3(VO_4)_2 + 4H_2SO_4 = (VO_2)_2SO_4 + 3CaSO_4 + 4H_2O \quad (14)$$

3.5. Pellet Performance Evaluation

In the pelletizing, roasting, acid leaching, and calcination processes, in order to meet the vanadium extraction process, requirements on the performance of pellets exist, accompanied by the loss of pellets in each stage. Under the optimum conditions, the compressive strength of the pellet during one roasting is 3283 N, the vanadium leaching rate is 74.51%, and the porosity is 28.73%. After acid leaching, the pellet strength is only almost 500 N. After secondary roasting of the pellets, the pellet strength can reach 2388 N. Table 2 shows the chemical composition of the secondary baked pellets. It can be seen from the table that the iron content in the pellets has increased. After vanadium extraction from iron concentrate, although a small amount of iron is leached, the impurity elements in the pellets will also be leached. Therefore, vanadium extraction indirectly improves the iron grade in the pellets, which is conducive to subsequent iron smelting. At the same time, there is a small amount of vanadium residue. In the future, oxidation roasting and improving the porosity of pellets can be considered to enhance the vanadium leaching effect.

Table 2. Chemical compositions (ICP) of secondary roasted pellet.

Element	Fe	Ti	Si	Ca	Mg	V	Al	Cr	Ni	Zn
Content (wt.%)	58.60	5.90	2.30	1.14	1.57	0.07	1.2	0.52	0.11	0.05

The raw ore, calcined pellets, acid leaching pellets, and secondary calcined pellets were analyzed by SEM-EDS. The distributions of Fe and V in Figure 8a are similar, which indicates that V in raw ore exists in Fe and V spinel. It can be seen from Figure 8b that V is relatively dispersed. This is relatively related to the distribution of Ca, which indicates that after roasting, vanadium reacts with calcium to generate calcium vanadate. In addition, V is not found in Figure 8c. This indicates that after sulfuric acid leaching, V in the pellet basically enters the leaching solution and S is observed, which indicates that there is some sulfur residue in the reaction process that is difficult to remove using physical methods. No sulfur is observed in Figure 8d, which indicates that the sulfur in the pellets is removed after secondary roasting.

Figure 9 shows the degree of damage on the surface of the pellets after different degrees of acid leaching. In (I), the surface of the pellets is slightly powdery after acid leaching. At this time, the properties of the pellets are relatively good. In (II), the pellets are slightly cracked, the pellet strength is low, and the pellet accumulation during acid leaching will cause a small portion of the pellets to break. In (III), the pellets were severely cracked, and a large amount of impurities entered the solution to increase the acid consumption. In (IV), the pellets not only cracked but also broke off due to the destruction of the pellet structure by acid leaching, resulting in a large amount of material entering the acid leach solution, which had a greater impact on the subsequent separation.

Figure 10 shows the relationship between the compressive strength of roasted pellets and the percentage of pellet porosity and the number of broken pellets after acid leaching. It can be seen that as the compressive strength of the pellets rises, the particle contact in the pellets becomes more compact and the pellet porosity decreases, with the decreasing trend of porosity leveling off when the pellet strength reaches about 3000 N. A large porosity can cause pellet breakage during acid leaching and a small porosity can cause difficulties in subsequent acid leaching for vanadium extraction. The percentage of damaged pellets after acid leaching reaches 81% when the strength of the roasted pellets is in the range of 0–1500 N. In the range of 1500–2000 N, the percentage of damaged amounts drops to approximately 60%. In the range of 2500–3500 N, the percentage of damaged particles decreases to 5% and the pellet handling is not easily broken after acid leaching. When the pellets reach 3500–4000 N, the pellets are less damaged, but at this point, the pellet porosity is too small for subsequent vanadium extraction. Under optimal roasting and acid leaching conditions, the pellet strength is 3288 N, at which time the pellet porosity is 15.28% and a few pellets are broken, which does not affect the secondary roasting.

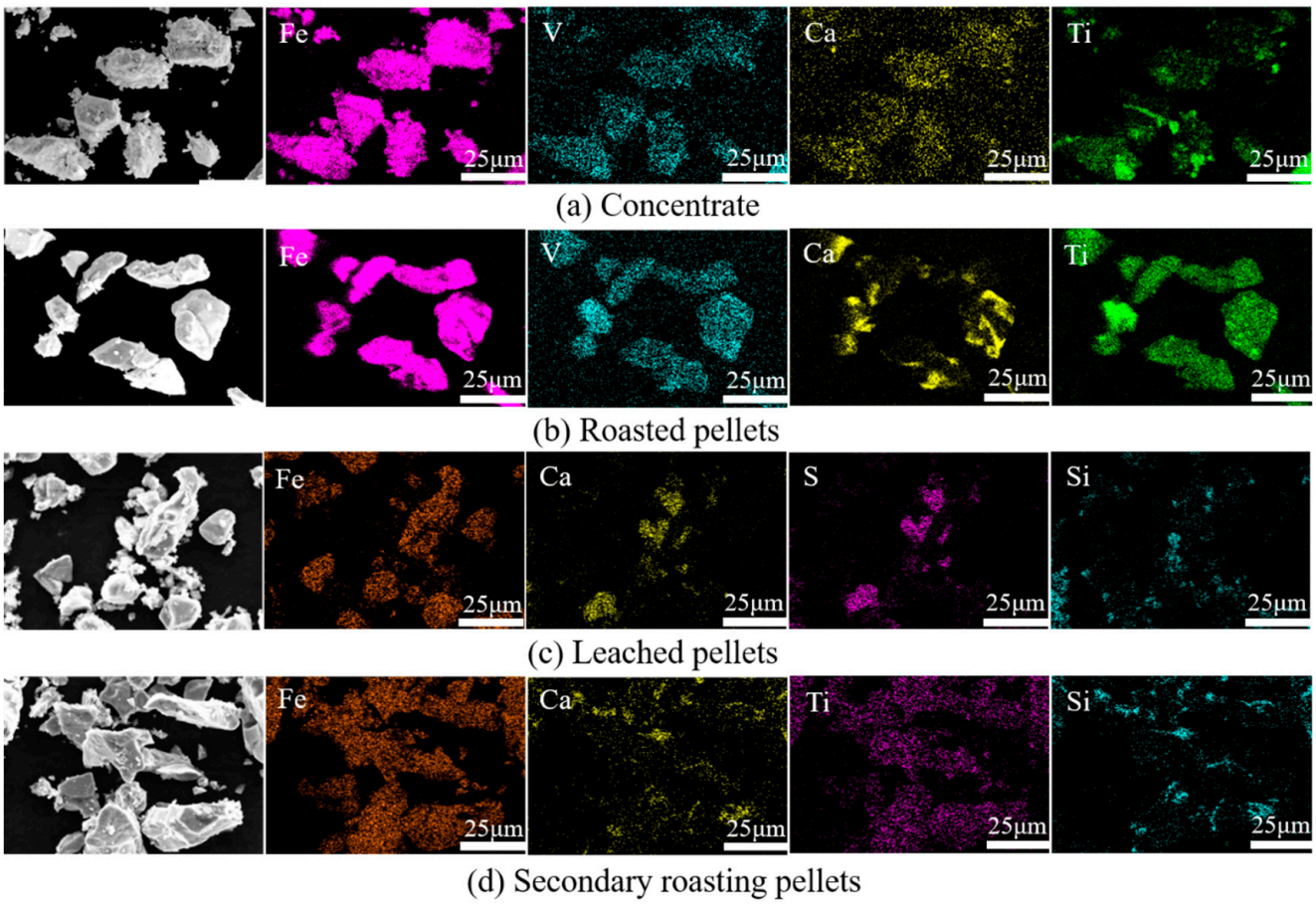


Figure 8. SEM images with EDS element mappings of iron ore concentrates at different stages. (**a**) EM-EDS analysis of concentrate; (**b**) EM-EDS analysis of roasted pellets; (**c**) EM-EDS analysis of leached pellets; (**d**) SEM-EDS analysis of secondary roasted pellets.

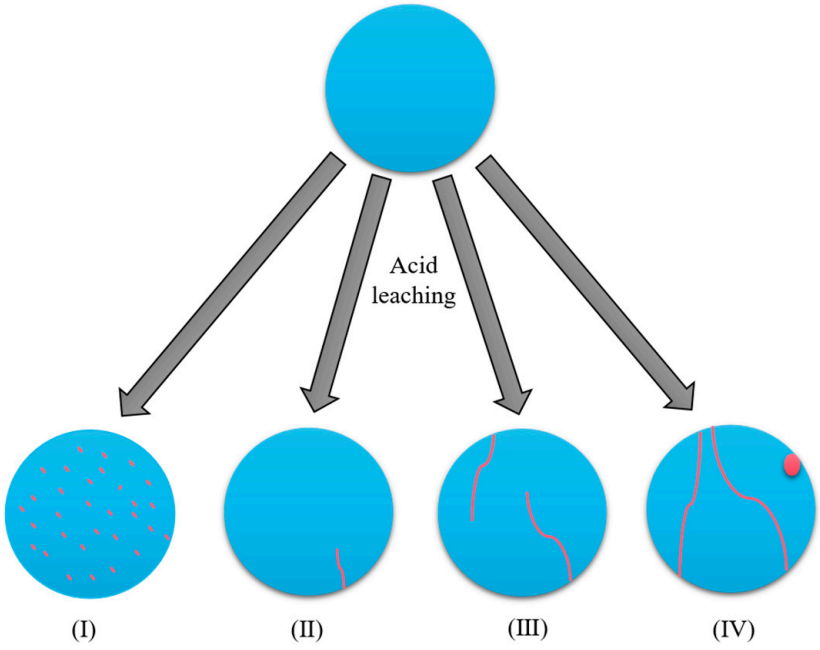


Figure 9. Diagram of the degree of breakage of pellets after acid leaching. (I) slightly powdery surface; (II) small crack: (III) servere: (IV)severe crushing.

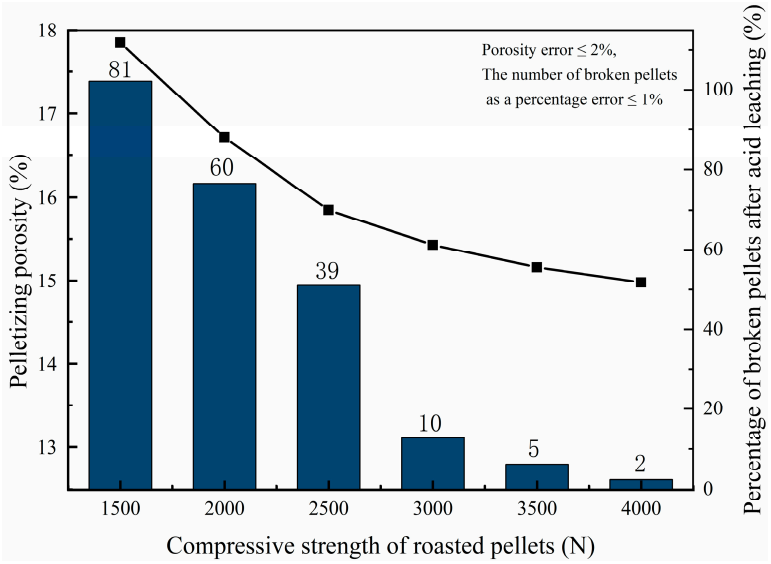


Figure 10. Effect of compressive strength of calcined pellets on properties of acid-leached pellets.

The experiments investigated the degree of damage and the percentage of broken pellets during the acid leaching process, which can further optimize the roasting and acid leaching experimental process parameters, balance the vanadium leaching rate and the performance of the pellets after leaching, and provide high-quality pellets for the secondary roasting.

4. Conclusions

The effects of the pelletizing process, roasting process, and acid leaching process on pellet performance and vanadium leaching rate were studied in this paper. The following conclusions are drawn.

The optimum pelleting conditions are −0.074 mm particle size, accounting for almost 80%, moisture content of 8% ± 1%, low addition of calcium hydroxide and bentonite, and a pelleting time of 19 min. Under these conditions, the falling strength of green pellets, compressive strength, bursting temperature, and pellet yield are the most suitable.

The best conditions for pellet roasting are a temperature of 1200 °C, 2 h roasting time, a calcium hydroxide ratio of 2%, and bentonite content of 0.8%. Under these conditions, the strength of the pellet can reach 3288 N, and its porosity is 15.28%. At this time, the pellet is most conducive to the subsequent vanadium extraction and has the highest performance. It can effectively and selectively separate vanadium, while iron is almost not leached, and the vanadium extraction rate is greater than 64.31%.

With sulfuric acid leaching, calcium vanadate in the pellet is selectively leached by reacting with sulfuric acid, while ferric iron cannot be leached by sulfuric acid. In addition, fewer impurities exist in the solution, and therefore the subsequent treatment is easier. The best process conditions are a sulfuric acid concentration of 3 mol/L, leaching temperature of 80 °C, time of 3 d, and liquid–solid ratio of 3:1. Under these conditions, the leaching rate of vanadium is 74.51%.

Author Contributions: Conceptualization, Y.L.; methodology, Y.L. and Z.P.; formal analysis, Y.L. and Z.W.; data curation, Y.L., Y.Z. and Z.P.; writing—original draft preparation, Y.L.; writing—review and editing, Y.L., Z.P., Z.W. and K.X.; funding acquisition, K.X. All authors have read and agreed to the published version of the manuscript.

Funding: This research received no external funding.

Data Availability Statement: Data are contained within the article.

Conflicts of Interest: The authors declare no conflict of interest.

References

1. Chen:, S.Y.; Fu, X.J.; Chu, M.S.; Liu, Z.G.; Jue, T. Life cycle assessment of the comprehensive utilisation of vanadium titanomagnetite. *J. Clean. Prod.* **2015**, *101*, 122–128. [CrossRef]
2. Liu, B.; Li, J.; Ren, Q.Q.; Cai, S.; Yang, X.; Zeng, Y.N.; Li, J.G. Leaching behavior and mineralogical evolution of vanadium released from sodium roasted-acid leaching tailing of vanadium slag. *J. Iron Steel Res. Int.* **2022**, *29*, 772–782. [CrossRef]
3. Ning, P.G.; Lin, X.; Wang, X.Y.; Cao, H.B. High-efficient extraction of vanadium and its application in the utilization of the chromium-bearing vanadium slag. *Chem. Eng. J.* **2016**, *301*, 132–138. [CrossRef]
4. Zhang, Y.; Zhou, J.P.; Sun, D.Q.; Li, H.M. Two pass laser welding of TC4 Titanium alloy to 301L stainless steel via pure V interlayer. *J. Mater. Res. Technol.* **2020**, *9*, 1400–1404. [CrossRef]
5. Yu, J.W.; Hu, N.; Xiao, H.X.; Gao, P.; Sun, Y.S. Reduction behaviors of vanadium-titanium magnetite with H_2 via a fluidized bed. *Powder Technol.* **2021**, *385*, 83–91. [CrossRef]
6. Lee, J.C.; Kurniawan; Kim, E.Y.; Chung, K.M.; Kim, R.; Jeon, H.S. A review on the metallurgical recycling of vanadium from slags: Towards a sustainable vanadium production. *J. Mater. Res. Technol.* **2021**, *12*, 343–364. [CrossRef]
7. Chen, H.; Zhang, X.Y.; Zhang, S.R.; Wu, S.X.; Chen, F.Y.; Xu, J.G. A comparative study of iron-vanadium and all-vanadium flow battery for large scale energy storage. *Chem. Eng. J.* **2022**, *429*, 132403. [CrossRef]
8. Wang, Z.H.; Chen, L.; Aldahrib, T.; Li, C.; Liu, W.Z.; Zhang, G.Q.; Yang, Y.H.; Luo, D.M. Direct recovery of low valence vanadium from vanadium slag-Effect of roasting on vanadium leaching. *Hydrometallurgy* **2020**, *191*, 105156. [CrossRef]
9. Gao, H.Y.; Jiang, T.; Xu, Y.Z.; Wen, J.; Xue, X.X. Change in phase, microstructure, and physical-chemistry properties of high chromium vanadium slag during microwave calcification-roasting process. *Powder Technol.* **2018**, *340*, 520–527. [CrossRef]
10. Zhang, G.Q.; Luo, D.M.; Deng, C.H.; Lv, L.; Liang, B.; Li, C. Simultaneous extraction of vanadium and titanium from vanadium slag using ammonium sulfate roasting-leaching process. *J. Alloys Compd.* **2018**, *742*, 504–511. [CrossRef]
11. Wen, J.; Jiang, T.; Zhou, W.Y.; Gao, H.Y.; Xue, X.X. A cleaner and efficient process for extraction of vanadium from high chromium vanadium slag: Leaching in $(NH_4)_2SO_4$-H_2SO_4 synergistic system and NH_4^+ recycle. *Sep. Purif. Technol.* **2019**, *216*, 126–135. [CrossRef]
12. Li, H.Y.; Wang, C.J.; Yuan, Y.H.; Guo, Y.; Diao, J.; Xie, B. Magnesiation roasting-acid leaching: A zero-discharge method for vanadium extraction from vanadium slag. *J. Clean. Prod.* **2020**, *260*, 121091. [CrossRef]
13. Liu, B.; Du, H.; Wang, S.N.; Zhang, Y.; Zheng, S.L.; Li, L.J.; Chen, D.H. A Novel Method to Extract Vanadium and Chromium from Vanadium Slag using Molten NaOH-$NaNO_3$ Binary System. *AIChE J.* **2013**, *59*, 541–552. [CrossRef]
14. Li, R.M.; Liu, T.; Zhang, Y.M.; Huang, J. Mechanism of Novel K_2SO_4/KCl Composite Roasting Additive for Strengthening Vanadium Extraction from Vanadium-Titanium Magnetite Concentrate. *Minerals* **2018**, *8*, 426. [CrossRef]
15. Zheng, H.Y.; Zhang, W.L.; Guo, Y.C.; Gao, G.J.; Shen, F.M. Transformation of Vanadium-Bearing Titanomagnetite Concentrate in Additive-Free Roasting and Alkaline-Pressure Leaching for Extracting Vanadium (V). *Minerals* **2019**, *9*, 197. [CrossRef]
16. Li, R.M.; Liu, T.; Zhang, Y.M.; Huang, J.; Xu, C.B. Efficient Extraction of Vanadium from Vanadium–Titanium Magnetite Concentrate by Potassium Salt Roasting Additives. *Minerals* **2018**, *8*, 25. [CrossRef]
17. Li, H.Y.; Fang, H.X.; Wang, K.; Zhou, W.; Yang, Z.; Yan, X.M.; Ge, W.X.; Li, Q.W.; Xie, B. Asynchronous extraction of vanadium and chromium from vanadium slag by stepwise sodium roasting–water leaching. *Hydrometallurgy* **2015**, *156*, 124–135. [CrossRef]
18. Wang, Z.H.; Zheng, S.L.; Wang, S.N.; Liu, B.; Wang, D.W.; Du, H.; Zhang, Y. Research and prospect on extraction of vanadium from vanadium slag by liquid oxidation technologies. *Trans. Nonferr. Metal Soc.* **2014**, *24*, 1273–1288. [CrossRef]
19. Shlewit, H.; Alibrahim, M. Extraction of sulfur and vanadium from petroleum coke by means of salt-roasting treatment. *Fuel* **2006**, *85*, 878–880. [CrossRef]
20. Zhang, X.F.; Liu, F.G.; Xue, X.X.; Jiang, T. Effects of microwave and conventional blank roasting on oxidation behavior, microstructure and surface morphology of vanadium slag with high chromium content. *J. Alloys Compd.* **2016**, *686*, 356–365. [CrossRef]
21. Wen, J.; Jiang, T.; Xu, Y.Z.; Cao, J.; Xue, X.X. Efficient extraction and separation of vanadium and chromium in high chromium vanadium slag by sodium salt roasting-$(NH_4)_2SO_4$ leaching. *J. Ind. Eng. Chem.* **2019**, *71*, 327–335. [CrossRef]
22. Luo, Y.; Che, X.K.; Cui, X.L.; Zheng, Q.; Wang, L. Selective leaching of vanadium from V-Ti magnetite concentrates by pellet calcification roasting-H_2SO_4 leaching process. *Int. J. Min. Sci. Technol.* **2021**, *31*, 507–513. [CrossRef]
23. Wong, G.J.; Fan, X.H.; Gan, M.; Ji, Z.Y.; Chen, X.L.; Tian, Z.Y.; Wang, Z.Z. Improvement on the thermal cracking performance of pellets prepared from ultrafine iron ore. *Powder Technol.* **2019**, *342*, 873–879. [CrossRef]
24. Zhang, J.H.; Zhang, W.; Zhang, L.; Gu, S.Q. Mechanism of vanadium slag roasting with calcium oxide. *Int. J. Mineral Process.* **2015**, *138*, 20–29. [CrossRef]
25. Zhang, S.H.; Li, G.H.; Xiao, R.D.; Luo, J.; Yi, L.Y.; Rao, M.J. Extraction of vanadium from low-vanadium grade magnetite concentrate pellets with sodium salt. *J. Mater. Res. Technol.* **2021**, *15*, 5712–5722. [CrossRef]

Disclaimer/Publisher's Note: The statements, opinions and data contained in all publications are solely those of the individual author(s) and contributor(s) and not of MDPI and/or the editor(s). MDPI and/or the editor(s) disclaim responsibility for any injury to people or property resulting from any ideas, methods, instructions or products referred to in the content.